THE JOURNAL OF BIOLOGICAL CHEMISTRY VOL. 289, NO. 19, pp. 13531–13542, May 9, 2014

Constitutive Expression of Pentraxin 3 (PTX3) Protein by Human Amniotic Membrane Cells Leads to Formation of the Heavy Chain (HC)-Hyaluronan (HA)-PTX3 Complex*

Received for publication, October 7, 2013, and in revised form, February 26, 2014 Published, JBC Papers in Press, March 20, 2014, DOI 10.1074/jbc.M113.525287

Suzhen Zhang[‡], Ying-Ting Zhu[‡], Szu-Yu Chen[‡], Hua He[‡], and Scheffer C. G. Tseng[‡§1]

From [‡]TissueTech, Inc., Miami, Florida 33173 and the [§]Ocular Surface Center, Miami, Florida 33173

Background: HC-HA from the amniotic membrane (AM) is produced by AM cells.
Results: Pentraxin 3 tightly binds to purified AM HC-HA and is constitutively secreted by AM cells, leading to HC-HA-PTX3 complex formation.
Conclusion: PTX3 is an integral component of AM HC-HA-PTX3 complexes.
Significance: HC-HA-PTX3, produced endogenously by the AM, may play an important protective role during fetal development and can be an active therapeutic agent.

Heavy chain (HC)-hyaluronan (HA), a complex formed by the covalent linkage between HC1 from the inter-α-trypsin inhibitor (IαI) and HA, purified from the human amniotic membrane (AM), is responsible for the anti-inflammatory, antiscarring, and antiangiogenic actions of the AM. This HC-HA complex is produced by constitutive expression of TNF-stimulated gene 6 and endogenous production of IαI by AM cells. Pentraxin 3 (PTX3), a prototypic long pentraxin that plays a non-redundant role in innate immunity against selected pathogens, also helps stabilize HC-HA to ensure female fertility. Here we noted strong positive PTX3 staining in the AM epithelium and compact stroma. PTX3 was constitutively expressed and secreted by cultured AM epithelial and stromal cells and, further, greatly up-regulated by TNF and IL-1β. Using an agarose overlay to trap the HA-containing matrix, the HC-HA-PTX3 complex was formed, as analyzed by Western blot analysis, by AM cells but not human skin fibroblasts, despite being cultured in the presence of serum and TNF. However, exogenous PTX3 helps human skin fibroblasts form the HC-HA-PTX3 complex with an agarose overlay. Furthermore, PTX3 can be coimmunoprecipitated with the HC-HA complex from agarose-overlaid AM cell extracts by an anti-human IαI antibody. Such a HC-HA-PTX3 complex can be reconstituted *in vitro* and exhibit similar effects as those reported for AM HC-HA-PTX3 on polarization of M2 macrophages. The tight binding between PTX3 and AM HC-HA withstands four runs of CsCl ultracentrifugation in the presence of 4 M GnHCl. These results indicate that PTX3 is constitutively expressed and secreted by AM cells as an integral component of the AM HC-HA-PTX3 complex and contributes to the biological function of AM HC-HA-PTX3.

Human pentraxin 3 (PTX3) is a 45-kDa glycoprotein that can form an octameric structure, *i.e.* a complex quaternary structure with eight protomer subunits held together by both covalent (disulfide) and non-covalent interactions (1). PTX3 is a member of long pentraxins that, together with short pentraxins such as C-reactive protein and serum amyloid P, form a group of soluble pattern recognition receptors as essential components of the innate immune system (2, 3). PTX3 shares with short pentraxins a C-terminal pentraxin-like domain that can bind with ligands, such as complement component C1q, microbial moieties galactomannan, and outer membrane protein A (a conserved constituent of the outer membrane of Enterobacteriaceae), selected microbes, apoptotic cells (4–6), and histones (7). Therefore, PTX3 acts as a soluble pattern recognition receptor in the innate immune response (2) and has a non-redundant protective role against selected pathogens, thus also possessing therapeutic benefits in several types of experimental infections (8–10).

Unlike C-reactive protein and serum amyloid P, which are produced by hepatocytes as "acute stress proteins" (11), PTX3 is produced by extrahepatic somatic and innate immunity cells, such as myeloid dendritic cells and macrophages (12), under inflammatory stimuli, such as Toll-like receptor engagement, TNF, and IL-1β. In addition, PTX3 holds a unique and unrelated N-terminal domain that binds with FGF2 (13), heavy chains (HCs)[2] of inter-α-trypsin inhibitor (IαI) or heavy chain-hyaluronan (HC-HA) (14), and TNF-stimulated gene 6 (TSG-6) (15). The HC-HA complex is a covalent complex formed by high molecular weight HA and HCs via an ester bond by a catalytic action of TSG-6 (16–18). Because the HC-HA complex is an integral component of the HA-rich matrix in the cumulus oophorus complex (COC) surrounding the oocyte (16, 19, 20), it is no wonder that infertility ensues in female *ptx3*-

* This work was supported, in whole or in part, by NEI, National Institutes of Health grants RO1 EY06819, R44 EY017497, and R43 EY021045 (to S. C. G. T.). This work was also supported by a research grant from TissueTech, Inc. and by an unrestricted grant from the Ocular Surface Research and Education Foundation (Miami, FL).

[1] To whom correspondence should be addressed: Ocular Surface Center, 7000 S.W. 97th Ave., Suite 213, Miami, FL 33173. Tel.: 305-274-1299; Fax: 305-274-1297; E-mail: stseng@ocularsurface.com.

[2] The abbreviations used are: HC, heavy chain; IαI, inter-α-trypsin inhibitor; HA, hyaluronan; COC, cumulus oophorus complex; AM, amniotic membrane; HAase, hyaluronidase; HABP, HA-binding protein; HMW, high molecular weight; AMEC, amniotic membrane epithelial cell(s); AMSC, amniotic membrane stromal cell(s); SHEM, supplemental hormonal epithelial medium; HSF, human skin fibroblast(s); rcHC, reconstituted heavy chain; SHAP, serum-derived hyaluronan-associated proteins.

deficient mice because of the lack of PTX3 that is important to stabilize HC-HA in the COC matrix (15).

From the human amniotic membrane (AM), we have isolated and characterized a HC-HA complex that exerts the anti-inflammatory, antiscarring, (21), and antiangiogenic (22) actions of AM. We have demonstrated that this HC-HA complex purified after ultracentrifugation contains only HC1, but not HC2, HC3, bikunin, and TSG-6, and is produced by cultured AM cells via constitutive expression of IαI and TSG-6 (23). Recently, we also demonstrated that such an AM HC-HA complex contains PTX3 and can polarize macrophages to an M2 phenotype upon Toll-like receptor ligation (24). Here we provide further evidence supporting the notion that PTX3 is indeed an integral component of such a purified AM HC-HA complex and is uniquely and constitutively expressed by AM cells, leading to extracellular accumulation of the HC-HA-PTX3 complex in the AM.

EXPERIMENTAL PROCEDURES

Materials—Guanidine hydrochloride, cesium chloride, EDTA, anhydrous alcohol, potassium acetate, sodium acetate, sodium chloride, sodium hydroxide, Tris base, Triton X-100, 3-(*N*,*N*-dimethyl palmitylammonio) propanesulfonate (Zwittergent$^{3-16}$), protease inhibitor mixture (including 4-(2-aminoethyl)-benzenesulfonyl fluoride hydrochloride, aprotinin, bestatin hydrochloride, E-64, leupeptin, and pepstatin A), DTT, protein A-Sepharose, and PMSF were obtained from Sigma-Aldrich (St. Louis, MO). *Streptomyces* hyaluronidase (HAase) and biotinylated HA-binding protein (HABP) were from Seikagaku Biobusiness Corp. (Tokyo, Japan). DMEM, Ham's F12 nutrient mixture, FBS, Hanks' balanced salt solution, gentamicin, amphotericin B, PBS, penicillin/streptomycin, enzyme-free cell dissociation buffer, radioimmune precipitation assay buffer, and agarose were purchased from Invitrogen. The Covalink-NH 96-well plate was from Nunc (Thermo Scientific, Rochester, NY). HMW HA (Healon) was purchased from Advanced Medical Optics (Santa Ana, CA). Select-HA HiLadder and Mega-HA Ladder were from Hyalose (Oklahoma City, OK). Slide-A-Lyzer dialysis cassettes (3.5 K MWCO) were from Fisher Scientific (Pittsburgh, PA). The BCA protein assay kit, sulfo-*N*-hydroxysuccinimide, 1-ethyl-3-(3-dimethylaminopropyl) carbidodiimide, and 1-Step Ultra TMB-ELISA substrate solution were from Pierce. The HA quantitative test kit was from Corgenix (Westminster, CO). 4–15% gradient acrylamide ready gels and nitrocellulose membranes were from Bio-Rad. IαI was prepared in our laboratory from human plasma according to the published method (25, 26). Recombinant human TNF, recombinant human Pentraxin 3/TSG-14, recombinant human TSG-6, and human/mouse TSG-6 mAb (catalog no. MAB2104) were from R&D Systems (Minneapolis, MN). PTX3 mAb (catalog no. MNB4) were from Enzo Life Sciences, Inc. (Plymouth, PA). Mouse anti-human ITIH1 polyclonal antibody against full-length ITIH1 and rabbit anti-human ITIH2 polyclonal antibody against amino acids 124–321 were from Abcam Inc. (Cambridge, MA). Rabbit anti-human IαI polyclonal antibody was from DAKO Corp. (Carpinteria, CA). The HiPerFect transfection reagent and RNeasy mini RNA isolation kit were from Qiagen (Valencia, CA). siRNA oligonucleotides for targeting endogenous human PTX3 (ACACUUGAGACUAAUGAAAGAGAGA) and non-targeting siRNA control oligonucleotides (scrambled RNA) were from OriGene Technologies, Inc. (Rockville, MD). Western Lighting™ chemiluminescence reagent was from PerkinElmer Life Sciences, Inc. (Waltham, MA). The RNeasy mini kit was from Qiagen. The high-capacity reverse transcription kit and primers (GAPDH and PTX3) for real-time PCR were from Applied Biosystems (Carlsbad, CA). ELISA kits for murine IL-10 and IL-12p40 were from Biolegend (San Diego, CA). The ultracentrifuge (LM8 model, SW41 rotor) was from Beckman Coulter, Inc. (Fullerton, CA).

Cell Cultures and Agarose Overlay—Human tissue was handled according to the Declaration of Helsinki. Fresh human placenta was obtained from healthy mothers after elective cesarean deliveries in the Baptist Hospital (Miami, FL) via approval (protocol no. 03-028) by the Baptist Health South Florida Institutional Review Board. Primary human AM epithelial and stromal cells (designated AMEC and AMSC, respectively) were isolated from fresh placenta as described previously (27, 28) and cultured in supplemental hormonal epithelial medium (SHEM), which consisted of DMEM/F12 (1:1, v/v), 5% (v/v) FBS, 0.5% (v/v) dimethyl sulfoxide, 2 ng/ml EGF, 5 μg/ml insulin, 5 μg/ml transferrin, 5 ng/ml sodium selenite, 0.5 μg/ml hydrocortisone, 0.1 nM cholera toxin, 50 μg/ml gentamicin, and 1.25 μg/ml amphotericin B (27, 29) under a humidified atmosphere of 5% CO_2 at 37 °C. Human skin fibroblasts (HSF) were cultured in the same condition as AMEC and AMSC. The culture medium was changed every 2 days. Cells at 80% confluence were switched to DMEM/F12 containing 0.5% FBS for 48 before being treated with 20 ng/ml of TNF or IL-1β for 4 or 24 h for quantitative PCR and Western blot analysis, respectively. For agarose overlay cultures, AMEC, AMSC, and HSF were seeded in 12-well or 6-well plates at a density of $2 \times 10^4/cm^2$ in SHEM to 80% confluence after attachment. After cell attachment, the medium was changed to FBS-free SHEM containing 5% knockout serum replacement and 1 mM 2-phospho-L-ascorbic acid after cells were washed three times with Hanks' balanced salt solution or changed to fresh FBS-containing SHEM and incubated for 2 days. After removal of the medium, 3% agarose (low melting type, type VII, Sigma, catalog no. A9045) in DMEM/F12 with 1 mM 2-phospho-L-ascorbic acid was overlayered at 0.5 ml or 1 ml to achieve a 1-mm-thick gel layer at room temperature for 5–10 min before adding FBS-free or FBS-containing SHEM medium with or without 5 ng/ml TNF. In some cases of agarose-overlaid HSF, 100 nM human recombinant PTX3 was added to the FBS-containing SHEM medium after the gel layer was formed. Cells were harvested, without changing the medium, on day 5.

siRNA Transfection—AMEC and AMSC were cultured in SHEM in 6-well plates till 80% confluence before being switched to DMEM/F12 with 0.5% FBS for 48 h and being transfected with 100 nM PTX3 siRNA or scrambled RNA with or without 20 ng/ml of TNF. After 48 h, cells were harvested and subjected to Western blot analysis.

Purification of the HC-HA Complex by Cesium Chloride Ultracentrifugation—The HC-HA complex was purified from the AM as described previously (21, 23, 30). In brief, cryopreserved human AM, obtained from Bio-Tissue, Inc. (Miami, FL),

was sliced into small pieces, frozen in liquid nitrogen, and ground to a fine powder by a BioPulverizer. The powder was mixed with cold PBS buffer at 1:1 (grams/milliliter). The mixture was kept at 4 °C for 1 h with gentle stirring and then centrifuged at 48,000 × *g* for 30 min at 4 °C. The supernatant (designated AM extract) was then mixed with an 8 M guanidine HCl/PBS solution (at a 1:1 ratio of v/v) containing 10 mM EDTA, 10 mM aminocaproic acid, 10 mM *N*-ethylmaleimide, and 2 mM PMSF, adjusted to a density of 1.35 g/ml, and subjected to isopycnic centrifugation at 35,000 rpm, 15 °C, for 48 h. The resultant density gradients were fractioned into 12 tubes (1 ml/tube) in which the contents of HA and proteins were measured using an HA quantitative test kit and BCA protein assay kit, respectively. Fractions from the first ultracentrifugation, which contained most HA, were pooled, brought to a density of 1.40 g/ml by addition of cesium chloride, ultracentrifuged, and fractionated in the same manner as described above. Fractions from the second ultracentrifugation, which contained HA but no detectable proteins, were pooled and continued to the third and fourth ultracentrifugation in a density of 1.42 g/ml by addition of cesium chloride. Fractions from the second and fourth ultracentrifugation were dialyzed in distilled water and then precipitated twice with 3 volumes of 95% (v/v) ethanol containing 1.3% (w/v) potassium acetate at 0 °C for 1 h. After centrifugation at 15,000 × *g*, the pellet was briefly dried by air, stored at −80 °C, and designated AM second HC-HA and fourth HC-HA, respectively.

Coimmunoprecipitation—AMSC with an agarose overlay were cultured in FBS-containing SHEM with 5 ng/ml TNF for 5 days as described above. After removing the agarose overlay and washing six times with cold PBS, the cells were lysed with radioimmune precipitation assay buffer at 4 °C for 1 h. The supernatants were collect after centrifugation at 14,000 × *g* for 30 min at 4 °C. A total of 1 mg of total proteins from the culture extracts was incubated for 1 h at 4 °C with protein A-Sepharose beads before being incubated with or without 20 units/ml of HAase for 1 h at 37 °C. They were then incubated with 50 μl of protein A-Sepharose beads and 10 μg of rabbit anti-human IαI antibody or rabbit preimmune IgG at 4 °C overnight. After incubation, the beads were washed five times with radioimmune precipitation assay buffer, and the bound material was eluted with 30 μl of 2× SDS sample buffer (125 mM Tris-HCl (pH 8.0), 4% SDS, 20% glycerol, and 100 mM DTT) by boiling at 100 °C for 10 min, followed by alkylation with iodoacetamide at 200 mM for 30 min at room temperature and addition of DTT to quench the reaction. Samples were analyzed by Western blot analysis.

Western Blot Analysis and Agarose Gel Electrophoresis—Culture supernatants were collected, and cell lysates were obtained by washing cells six times with cold PBS, followed by incubating in radioimmune precipitation assay buffer at 4 °C for 1 h for cells without agarose overlay or incubating in 6 M guanidine HCl, 0.2 M Tris-HCl (pH 8.0), 0.1% (w/v) Zwittergent$^{3-16}$ buffer containing 10 mM EDTA, 10 mM aminocaproic acid, 10 mM *N*-ethylmaleimide, and 2 mM PMSF at 4 °C overnight (23, 31) for cells with agarose overlay, with gentle stirring and centrifugation at 14,000 × g for 30 min at 4 °C. Protein concentrations in culture supernatants and cell lysates were quantified with a BCA protein assay kit. Samples were incubated in 50 mM NaOH for 1 h at 25 °C or dissolved in 0.1 M sodium acetate buffer (pH 6.0) and incubated at 60 °C for 1 h with or without 20 units/ml of *Streptomyces* HAase. They were then resolved by SDS-PAGE on 4–15% (w/v) gradient acrylamide ready gels under denaturing and reducing conditions with the presence of 2% SDS and 5% 2-mercaptoethanol and transferred to a nitrocellulose membrane. For reduction and alkylation prior to SDS-PAGE, samples of AM extract or AM HC-HA complex treated with or without NaOH or HAase were mixed with an equal volume of 2× SDS sample buffer (125 mM Tris-HCl (pH 8.0), 4% SDS, 20% glycerol, and 100 mM DTT) and incubated for 10 min at 100 °C, followed by alkylation with iodoacetamide at 200 mM for 30 min at room temperature and addition of DTT to quench the reaction. The membrane was then blocked with 5% (w/v) fat-free milk in 50 mM Tris-HCl (pH 7.5) buffer containing 150 mM NaCl and 0.05% (v/v) Tween 20, followed by sequential incubation with different primary antibodies and their respective HRP-conjugated secondary antibodies. Immunoreactive proteins were visualized by Western Lighting^{TM} chemiluminescence reagent. For coimmunoprecipitation, the immunoblot was first probed with anti-human IαI antibody and then stripped and reprobed with anti-human PTX3 antibody. For agarose gel electrophoresis of the AM HC-HA complex, samples with or without HAase digestion were separated on 0.5% (w/v) agarose gels, followed by staining with 0.005% (w/v) Stains-all dye in 50% (v/v) ethanol. The gels were stained overnight at 25 °C with light protection, and HA was visualized as bluish bands after destaining in water and exposure to room light for 6 h. The Select-HA HiLadder and Mega-HA Ladder mixture was used as an HA marker and HMW HA (Healon) as a positive control.

Immunostaining—Human fetal membranes containing AM and chorion sections were fixed with 4% paraformaldehyde for 15 min at room temperature, followed by washing with PBS. Cell cultures with an agarose overlay were fixed in 4% paraformaldehyde with the agarose overlay for 15 min at room temperature. The agarose layer was removed before washing with PBS. After permeabilizing with 0.2% (v/v) Triton X-100 in PBS for 20 min, the sections and cells were blocked with 0.2% (w/v) bovine serum albumin in PBS for 1 h and incubated with biotinylated HABP (for HA, 5 μg/ml), anti-PTX3, anti-HC1, or anti-HC2 antibodies (all diluted 1:200 in blocking solution) overnight in a humidity chamber at 4 °C. After washing with PBS, they were incubated with Alexa Fluor 555-conjugated streptavidin (for HA, diluted 1:100) or respective secondary antibodies (*i.e.* Alexa Fluor 488-conjugated anti-mouse IgG, Alexa Fluor 488-conjugated anti-rat IgG, or Alexa Fluor 488-conjugated anti-rabbit IgG) for 1 h at room temperature. Isotype-matched, nonspecific IgG antibodies were used as a control. Alternatively, sections and cells were treated with 50 units/ml *Streptomyces* HAase at 37 °C for 4 h before fixation. Nuclei were stained by Hoechst 33342, and images were obtained using a Zeiss LSM700 confocal laser-scanning microscope (Zeiss, Germany).

Reconstitution of the HC-HA and HC-HA-PTX3 Complex (rcHC-HA and rcHC-HA-PTX3) in Vitro—The reconstitution of rcHC-HA and rcHC-HA/PTX3 was performed as described

previously (21, 24, 32) with minor modifications. In brief, HA was initially covalently cross-linked to Covalink-NH 96-well plates (2 μg/well) at 4 °C for 16 h, and the unbound HA was removed by washing with PBS containing 2 M NaCl and 50 mM $MgSO_4$, followed by PBS. The wells were then blocked with 2% BSA in PBS containing 0.1% Tween 20 (PBST) at room temperature for 1 h followed by washing with PBST. Thereafter, 200 nM purified human IαI (220 kDa) and 200 nM recombinant human TSG-6 (30.5 kDa) were mixed in PBST containing 5 mM $MgSO_4$ with or without 20 nM, 100 nM, or 200 nM of recombinant human PTX3 (41 kDa) and coincubated in the wells with or without immobilized HA for 2 h at 37 °C. The wells were washed three times with PBST and then three times with 6 M GnHCl. AM fourth HC-HA/PTX3 (2 μg/well) were coupled to the Covalink-NH 96-well plates as a positive control. To determine the bound components on immobilized HA, the wells were blocked with 2% BSA in PBS for 1 h at room temperature and incubated with anti-HC1 antibody, anti-TSG-6 antibody, anti-PTX3 antibody, or anti-HC2 antibody (all with a 1:1000 dilution in 2% BSA) for 2 h at room temperature, followed by incubation with a horseradish peroxidase-conjugated anti-mouse, anti-rat, or anti-rabbit immunoglobulin antibody (dilution 1:1000 in 2% BSA). After incubation with 1-Step Ultra TMB-ELISA substrate solution and stop solution, the absorbance at 450 nm was read with 650 nm as a reference.

Macrophage Phenotype Assay—The assay was carried out as reported previously (24). Murine macrophage RAW264.7 cells were cultured in DMEM with 10% FBS, 100 units/ml penicillin, and 100 μg/ml streptomycin on plastic. After washing with PBS, resting RAW264.7 cells were harvested by enzyme-free cell dissociation buffer, treated with or without 1 μg/ml LPS, and immediately seeded on the wells (3.1×10^4/cm^2) with or without rcHC-HA and rcHC-HA/PTX3, as described above. After incubation for 24 h at 37 °C, the medium was collected for a cytokine ELISA assay according to the instructions of the manufacturer.

Real-time PCR—Total RNA was extracted from cell cultures using an RNeasy mini RNA isolation kit. The cDNA was reverse-transcribed using a high-capacity reverse transcription kit and amplified by quantitative PCR using specific primer-probe mixtures and DNA polymerase in a 7300 real-time PCR system (Applied Biosystems, Foster City, CA). GAPDH gene expression was used to normalize the amounts of the amplified products.

Statistical Analysis—The data are reported as the mean ± S.D. of four independent experiments. Statistical analysis was evaluated with Student's *t* test. $p < 0.05$ was considered to be statistically significant.

RESULTS

Presence of PTX3 in AM Epithelium and Compact Stroma—Immunofluorescence staining using an anti-human PTX3 antibody was performed on cross-sections of fresh human fetal membrane, which consisted of a simple epithelium and an avascular stroma, of which the latter could be further discerned histologically into a compact layer and a spongy layer and the subjacent cell-rich chorion (Fig. 1, *Phase*). Positive PTX3 staining was not only found in the apical surface of the epithelium, as

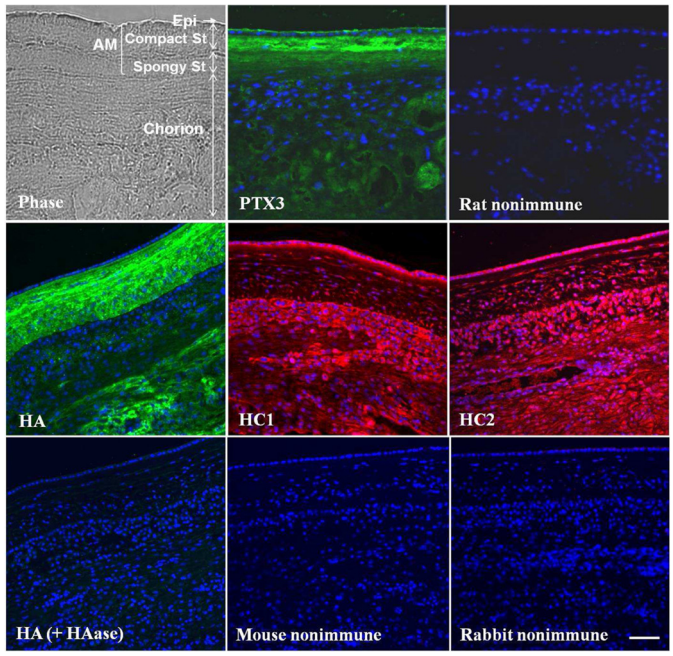

FIGURE 1. **Immunolocalization of PTX3 in the human AM.** Frozen sections of a human fetal membrane containing the amnion and the chorion were probed with rat anti-PTX3, mouse anti-HC1, or rabbit anti-HC2 antibodies and Alexa Fluor 488-conjugated anti-rat, Alexa Fluor 488-conjugated anti-mouse, or Alexa Fluor 488-conjugated anti-rabbit IgG secondary antibodies (*green*) or probed with biotinylated HABP with or without HAase digestion and Alexa Fluor 555-conjugated streptavidin (*red*). Non-immune rat or mouse IgG or non-immune rabbit serum was used as a control. Nuclei were counterstained with Hoechst 33342 (*blue*). *Epi*, epithelium; *St*, stroma. *Scale bar* = 100 μm.

reported previously (33), but was also more noticeable in the compact stroma (Fig. 1, *PTX3*). In contrast, PTX3 staining was markedly attenuated in the spongy stroma and the chorion and could not be unmasked by HAase digestion (data not shown). Consistent with our recent report (23), positive HA immunostaining using biotinylated HABP was more intense in the AM stroma than in the AM epithelium and the chorion (Fig. 1, *HA*). Such positive HA staining was specific to HA because it disappeared when the tissue section was predigested by HAase (Fig. 1, *HA (+HAase)*). Positive immunostaining to each individual HC was also noted in the AM epithelium, stromal cells, matrix, and chorion (Fig. 1, *HC1* and *HC2*). The staining described above is specific as judged by the lack of immunoreactivity by a non-immune control. These results suggest the predominant presence of PTX3 in the AM compact stroma and epithelium.

Presence of PTX3 in the AM Soluble Extract and Purified HC-HA Complex—To substantiate the presence of PTX3 in the AM, we performed Western blotting analyses of the AM extract obtained by an isotonic salt buffer before and after 50 mM NaOH treatment to cleave ester bonds (21, 23, 34, 35). Recombinant PTX3 appeared as a major 45-kDa species and a minor 90-kDa species corresponding to the native PTX3 monomer and dimer (Fig. 2*A*, *lane 2*). The soluble AM extract revealed 45-kDa, a 90-kDa, and a HMW species at the bottom of the loading well (mostly not entering the gel) and a minor 180-kDa species (Fig. 2*A*, *lane 3*). NaOH treatment did not affect the 45-kDa and 90-kDa species but completely eliminated the HMW species, resulting in an HMW smear of PTX3 (Fig. 2*A*, *lane 4*). These results suggest that PTX3 exhibited as a mono-

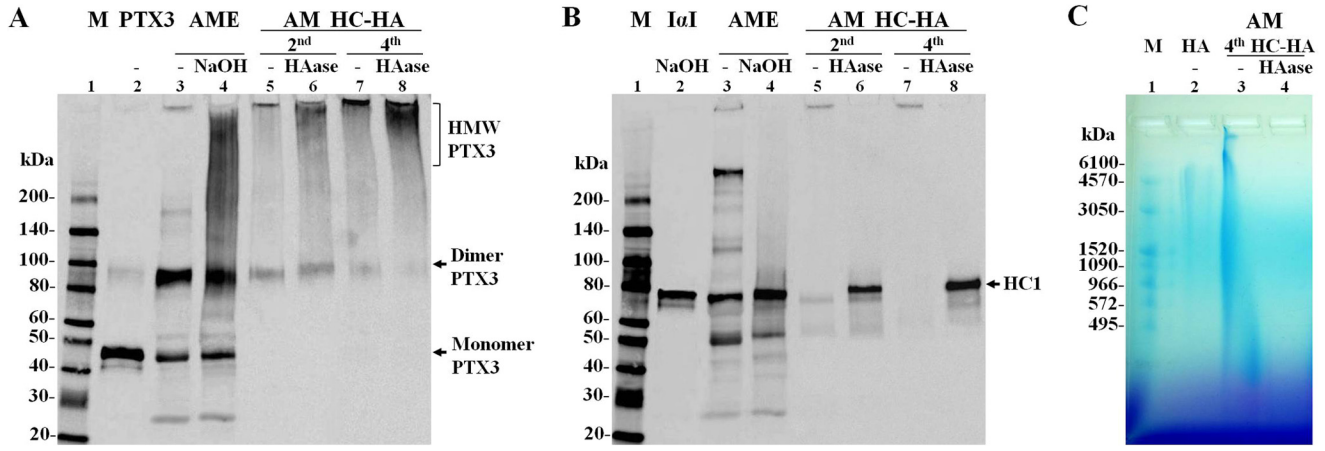

FIGURE 2. **Presence of PTX3 in both AM soluble extract and the purified HC-HA complex.** *A* and *B*, recombinant human PTX3 control, purified human IαI control, AM extract (*AME*) and the AM HC-HA complex were treated with or without 50 mM NaOH at 25 °C for 1 h or HAase at 37 °C for 1 h and separated by 4–15% SDS-PAGE. The control of PTX3 and the control of IαI (after NaOH treatment) were mixed just before loading to the same well of the gel. The immunoblot was first probed with rat anti-PTX3 antibody (*A*) and then stripped and reprobed with mouse anti-HC1 antibody (*B*). *M*, protein ladder markers. *C*, the AM HC-HA complex with or without HAase digestion was separated by 0.5% agarose gel, followed by staining with 0.005% Stains-all dye overnight at 25 °C with light protection. HA was visualized as *bluish bands* after destaining in water and exposure to room light for 6 h. HMW HA was used as a positive control. *M*, HA ladder markers.

mer, dimer, and HMW complex in the soluble AM extract in the presence of SDS, reduction by DTT, and alkylation by iodoacetamide. The HMW complex existed despite 50 mM DTT/200 mM iodoacetamide (Fig. 2*A*), 10 mM DTT/50 mM iodoacetamide, and 5 mM tributylphosphine/15 mM iodoacetamide (not shown). The HMW PTX3-containing species in the loading well was likely associated with the HC-HA complex because NaOH cleaves off the ester covalent linkage between HC and HA in the HC-HA complex (21, 31, 35). To further confirm this notion, we purified the HC-HA complex by two and four successive runs of ultracentrifugation from the AM soluble extract, as reported previously (21, 23), and subjected it to Western blot analyses with or without HAase digestion. Contrasting with both the monomer and dimer found in the soluble AM extract, a 90-kDa PTX3 dimer was noted in AM second and fourth HC-HA complex besides an HMW band at the bottom of the loading well (Fig. 2*A*, *lanes 5* and *7*). In addition, an HMW smear appeared in the second HC-HA and fourth HC-HA complex, with the latter being stronger. After HAase treatment, the 90-kDa dimer remained in both HC-HA complexes, but the HMW smear was intensified in the fourth HC-HA complex more than in the second HC-HA with the disappearance of the HMW band in the loading well (Fig. 2*A*, *lanes 6* and *8*), similar to the result seen in the AM extract. Elimination of DTT from the sample buffer resulted in the absence of this 90-kDa species in the AM HC-HA complex with or without HAase (data not shown). It has been reported that PTX3 protomer subunits are assembled into covalent octamers through interchain disulfide bonds and that PTX3 oligomerization is essential for its function in cumulus matrix organization and stabilization, where PTX3 interacts with HCs of HC-HA via its N-terminal domain (1, 36). The above results suggest that the HMW PTX3 smear was not an artifact because of reoligomerization and that PTX3 in the HC-HA complex most likely existed as an octamer.

In agreement with our previous report (21, 23, 24), Western blot analysis with an anti-HC1 antibody after stripping of PTX3 confirmed that the AM extract contained an HC-HA complex which as an HMW species present in the loading well, IαI (250 kDa) and free HC1 (75 kDa) (Fig. 2*B*, *lane 3*), and NaOH treatment lead to the disappearance of the HMW HC-HA complex and IαI resulting in the increase of HC1 (Fig. 2*B*, *lane 4*). The purified HC-HA complex displayed as an HMW species at the bottom of the loading well and disappeared upon HAase digestion (Fig. 2*B*, *lanes 5–8*). Furthermore, HC1 was released from the HC-HA complex after HAase digestion (Fig. 2*B*, *lanes 6* and *8*). A free 80-kDa HC1 band was detected only in the second HC-HA complex (Fig. 2*B*, *lane 6*) but not in the fourth HC-HA complex, suggesting that the latter did not contain free HC1. The presence of HA in the fourth HC-HA complex was verified by agarose gel electrophoresis as a continuous HA smear from the top loading well to the bottom of the gel that disappeared after HAase digestion (Fig. 2*C*). These results collectively suggest that the HC-HA complex purified from the AM, indeed, was strongly bound to PTX3 to form the HC-HA-PTX3 complex, despite four ultracentrifugations in the presence of cesium chloride and 4 M GnHCl, and that this HC-HA-PTX3 complex only contained HC1.

Biosynthesis of PTX3 by AMEC and AMSC—Cultured HSF were reported to express PTX3 mRNA and protein only under the stimulation of proinflammatory cytokines such as TNF and IL-1 (37–39). Thus, we wanted to compare the expression of PTX3 by AMEC and AMSC, cultured as described previously (23, 27, 28), to that by HSF. As expected, quantitative PCR showed that the expression of the PTX3 transcript was low in resting HSF but up-regulated by TNF and IL-1β 4.1-fold and 2.0-fold, respectively (Fig. 3*A*). Although the expression of the PTX3 transcript in resting AMEC and AMSC was also low, it was elevated dramatically by TNF or IL-1β to 37.6-fold and 39.1-fold in AMEC as well as 143.9-fold and 124.2-fold in AMSC, respectively (Fig. 3*A*). The 45-kDa PTX3 protein band was detected in a small amount in lysates but undetectable in the medium of resting HSF by Western blot analysis (Fig. 3*B*, *lane 2*). However, the amount of PTX3 protein was increased only slightly in lysates and remained undetectable in the

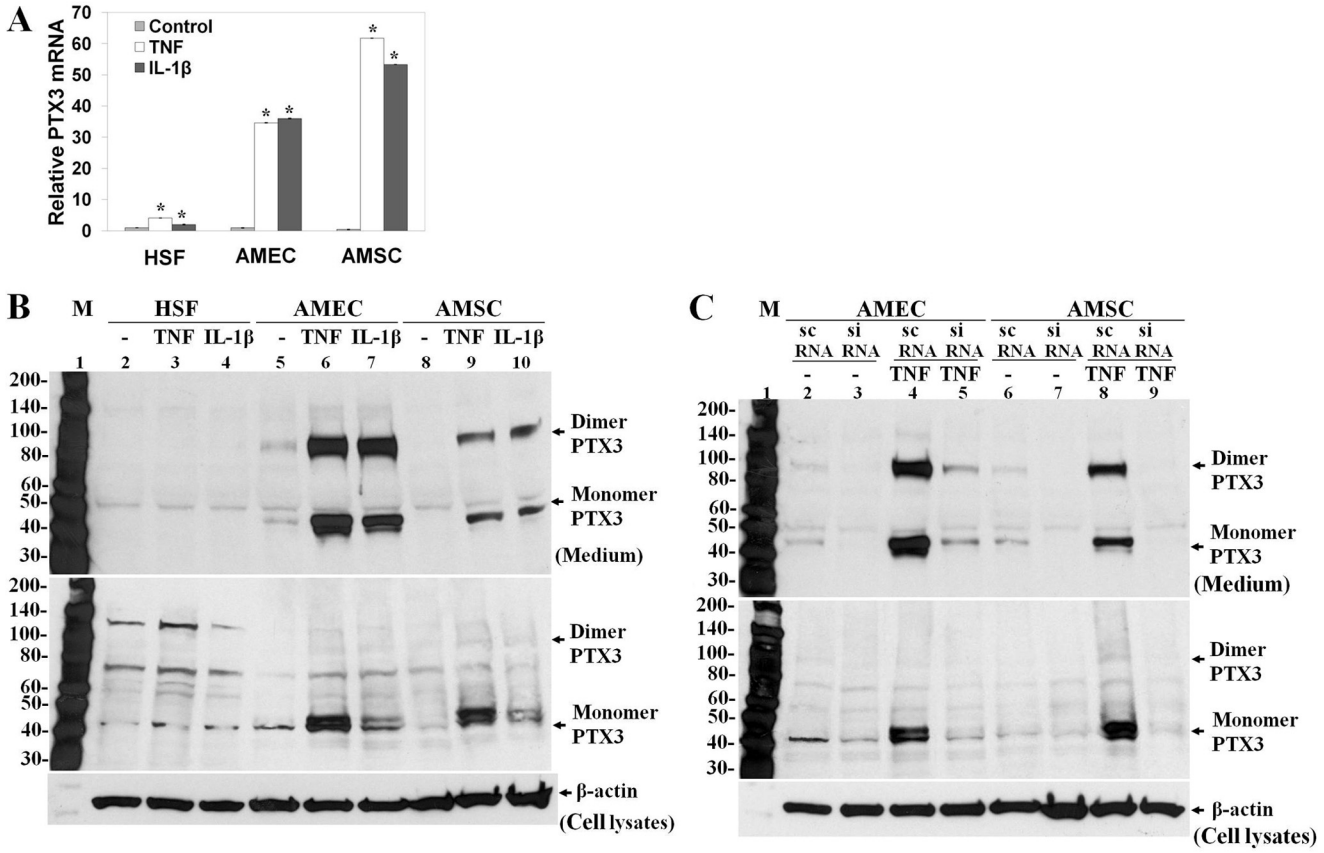

FIGURE 3. **Expression of PTX3 mRNA and protein by AMEC and AMSC.** Total RNAs and proteins were extracted from HSF, AMEC, and AMSC cultured in DMEM/F12 with 0.5% FBS for 48 h before being treated with 20 ng/ml of TNF or IL-1β for 4 h (real-time PCR) or 24 h (Western blot analysis). *A*, the expression of PTX3 mRNA was analyzed by real-time PCR with GAPDH as the endogenous control. *, $p < 0.01$, statistically significant groups in comparison with the control. *B*, the expression of PTX3 protein in medium (*top panel*) and cell lysates (*center panel*) was compared by Western blot with anti-PTX3 antibody and normalized by the β-actin control. *M*, protein ladder markers. *C*, PTX3 siRNA transfection was performed in AMEC and AMSC with or without 20 ng/ml of TNF after being cultured in DMEM/F12 with 0.5% FBS for 48 h. The down-regulation of PTX3 in both medium (*top panel*) and cell lysates (*center panel*) by PTX3 siRNA was verified by Western blot analysis. *scRNA*, scrambled RNA; *M*, protein ladder markers.

medium of HSF after addition of TNF or IL-1β for 24 h (Fig. 3*B*, *lanes 3* and *4*). In contrast, PTX3 protein was readily detectable in both lysates (45 kDa) and medium (45 kDa and 90 kDa) in resting AMEC and increased notably by TNF or IL-1β (Fig. 3*B*, *lanes 5*, *6*, and *7*), with TNF being more potent than IL-1β. The same finding was noted in AMSC (Fig. 3*B*, *lanes 8*, *9*, and *10*). Both 75-kDa and 135-kDa bands in lysates and the 50-kDa band in media of these three types of cells were nonspecific because they did not change under TNF or IL-1β. Furthermore, they did not change by PTX3 siRNA transfection, which, nonetheless, effectively down-regulated the 45-kDa PTX3 monomer in lysates and both the 45-kDa monomer and 90-kDa dimer of PTX3 in the media of both AMEC and AMSC cultures (Fig. 3*C*). These results collectively suggest that synthesis and secretion of PTX3 took place and was further up-regulated by proinflammatory stimuli in resting AM cells but not HSF.

Production of HC-HA-PTX3 Matrix by AM Stromal Cells—Previous studies have shown that another HC-HA complex, termed SHAP-HA, can be isolated from the cell layer of cultured mouse dermal fibroblasts in a medium supplemented with FBS and that such isolated HC-HA contains both HC1 and HC2 of IαI derived from FBS (31, 40). In contrast, we reported that the HC-HA complex can be produced by AM cells cultured in a serum-free medium because of their constitutive expression of endogenous IαI (23). Now that AMEC and AMSC constitutively synthesized and secreted PTX3 protein, we aimed to determine whether they produced the HC-HA complex that also contained PTX3. We also wanted to know whether HSF, which expressed PTX3 only under proinflammatory stimuli, *e.g.* TNF and IL-1 (Fig. 3), could also produce the HC-HA-PTX3 complex. To prevent the HA-containing matrix from being released into the medium, we overlaid 3% agarose on confluent cultures, a maneuver that was deployed by others to entrap secreted procollagens at or near the cell surface (41, 42). Without an agarose overlay, the HA ELISA assay showed that the HA level was readily detected in the serum-free medium of all three confluent cultures and increased significantly by TNF in both AMSC and AMEC but not HSF cultures (Fig. 4*A*). The same trend was noted but further promoted in the FBS-containing medium. Agarose overlay reduced the HA level in the medium more than 50% in both FBS-free and FBS-containing conditions in all three cultures. In all instances, AMSC produced much more HA than HSF and AMEC. After 5 days of agarose overlay, HSF, AMSC, and AMEC became more compact, especially in the FBS-containing condition. The epithelial morphology of AMEC became more evident (Fig. 4*B*). These results suggest that the agarose overlay was effective in reducing the release of HA

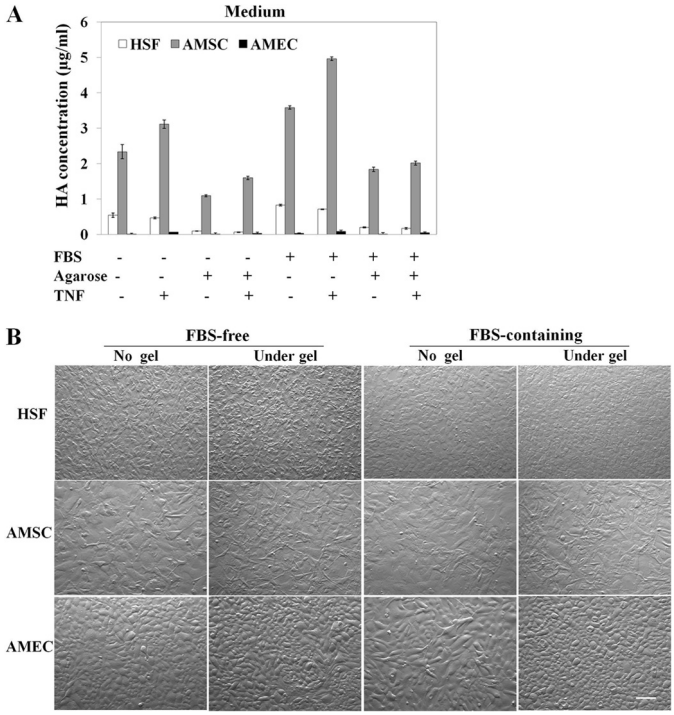

FIGURE 4. **Agarose overlay reduces HA release into the medium.** *A*, the HA concentration measured by ELISA assay was reduced in culture media from HSF, AMSC, and AMEC following agarose overlay for 5 days in both serum-free and FBS-containing conditions when compared with that without agarose overlay. *B*, phase-contrast micrographs of HSF, AMSC, and AMEC cultured in both FBS-free and FBS-containing conditions with or without agarose overlay for 5 days. *Scale bar* = 50 μm.

into the culture medium and could be used to entrap the HA-containing matrix to the cell layer.

We then performed double immunostaining for PTX3-HA, HC1-HA, and HC2-HA using biotin-labeled HABP, specific antibodies to HC1 and HC2, and anti-PTX3 antibody, respectively, to examine the aforementioned HA-containing matrix trapped to the cell layer by agarose overlay. In the FBS-containing HSF culture, positive HA staining was noted in the pericellular region, whereas PTX3 staining was negative (Fig. 5*A*). Addition of TNF yielded positive PTX3 staining in cells without a noticeable increase of the HA staining. A similar result was noted in the serum-free HSF culture (data not shown). In contrast, strong positive HA staining as a fibrillar network was noted on the cell surface and positive PTX3 staining in cells in resting (Fig. 5*A*) and TNF-treated (not shown) AMSC without FBS (Fig. 5*A*). In the resting and TNF-treated serum-free AMEC culture, strong positive HA staining appeared as fibrils only in sporadic extracellular spaces where cells were not as confluent and positive PTX3 staining in cells (Fig. 5*A*). A similar result was noted in both FBS-containing AMSC and AMEC cultures (data not shown). These results further confirm that PTX3 was constitutively expressed by AMSC and AMEC but not HSF. Positive HC1 or HC2 staining was noted in HSF only in the presence of FBS, which provides IαI, with (Fig. 5*B*) or without (not shown) TNF treatment. In contrast, such positive staining for HC1 and HC2 was found in AMSC and AMEC even in the absence of FBS and TNF treatment (Fig. 5*B*). Collectively, these results support the notion that the extracellular HA-rich matrix was trapped by the agarose overlay in these cell cultures.

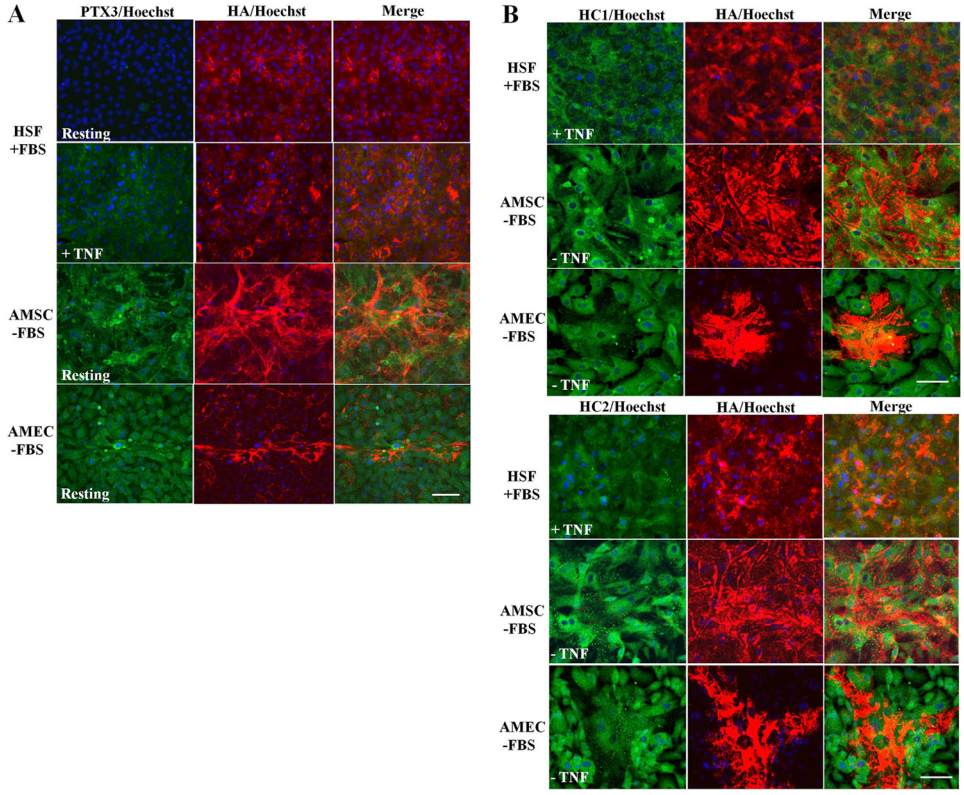

FIGURE 5. **Immunolocalization of HA, PTX3, HC1, and HC2 in cells cultured under agarose overlay.** HSF, AMSC, and AMEC were cultured with an agarose overlay with or without TNF treatment for 5 days. Cells were probed for hyaluronan (*red*), PTX3 (*green*), HC1 (*green*), and HC2 (*green*). Nuclei were counterstained with Hoechst 33342 (*blue*). *Scale bar* = 50 μm.

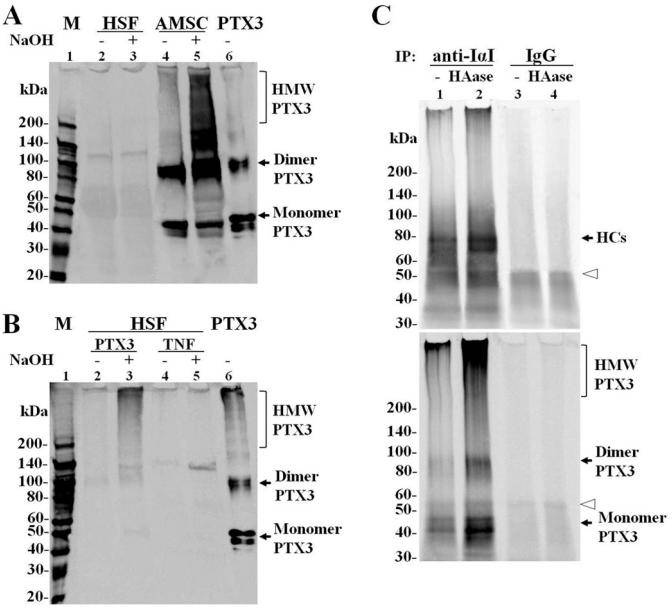

FIGURE 6. **The HC-HA-PTX3 complex formed by AMSC with endogenous PTX3 and by HSF with exogenous PTX3.** *A*, GnHCl extracts of cell layers from agarose-overlaid HSF and AMSC cultures in the presence of FBS and TNF were subjected to Western blot analysis for PTX3 with or without NaOH treatment. Recombinant PTX3 was used as a positive control. An HMW PTX3 smear was only present in AMSC but not HSF, even in the presence of FBS and TNF. *M*, protein ladder markers. *B*, exogenous PTX3 helped HSF form an HMW PTX3 smear in the presence of FBS without TNF. HSF were cultured under an agarose overlay in FBS-containing medium with 100 nM human recombinant PTX3 or 5 ng/ml TNF for 5 days, and then the GnHCl extracts were subjected to Western blot analysis for PTX3. *C*, agarose-overlaid AMSC culture extracts with or without HAase digestion was first immunoprecipitated (*IP*) with rabbit anti-IαI antibody or control rabbit IgG and separated by 4–15% SDS-PAGE. The immunoblot was then probed with rabbit anti-human IαI polyclonal antibody (*top panel*), stripped, and reprobed with rat anti-human PTX3 monoclonal antibody (*bottom panel*). The *open arrowheads* indicate heavy chains of rabbit IgG linked to the Sepharose beads and eluted by denaturation of the beads in sample buffer.

To test whether the HC-HA-PTX3 complex was produced by AMSC, we extracted cell layers with 6 M GnHCl and performed a Western blot analysis from AMSC and HSF cultured under agarose overlay in a FBS-containing medium and treated with TNF, a condition that allowed HSF to produce PTX3 (Fig. 5*A*) and an HC-HA complex (31). Under this condition, PTX3 was not detected in HSF with or without NaOH treatment (Fig. 6*A*, *lanes 2* and *3*, the faint 120-kDa species was nonspecific). In contrast, PTX3, appearing as an HMW PTX3 smear, 90-kDa dimer, and 45-kDa monomer, was readily detected in AMSC (Fig. 6*A*, *lane 4*). Furthermore, the HMW PTX3 smear was increased greatly by NaOH treatment (Fig. 6*A*, *lane 5*), which breaks the ester linkage between HCs and HA, leading to dissolution of HC-HA (21, 35, 43), suggesting that HMW PTX3 was released from the HC-HA complex. These results confirmed that AMSC, but not HSF, produced the HC-HA-PTX3 complex by constitutive production of PTX3. To verify that the formation of the HC-HA-PTX3 complex required extracellular PTX3, we applied exogenous recombinant human PTX3 in agarose-overlaid HSF in the same FBS-containing condition. An HMW PTX3 smear was generated by exogenous PTX3 in resting HSF without TNF (Fig. 6*B*, *lane 2*), and its intensity was increased greatly by NaOH (Fig. 6*B*, *lane 3*). This result resembled what was shown in AMSC (Fig. 6*A*, *lane 5*) and suggested that the exogenous HMW PTX3 was tightly bound to an HC-HA complex and was released when the ester bond was cleaved by NaOH. Importantly, TNF treatment alone without exogenous PTX3 did not generate such an HMW PTX3 smear (Fig. 6*B*, *lanes 4* and *5*). These results verified that extracellular PTX3 was responsible for the formation of the HC-HA-PTX3 complex.

To further verify the interactions between PTX3, HCs, and HA in agarose-overlaid cell cultures, we first used an anti-human IαI antibody to immunoprecipitate complexes from AMSC culture extracts with or without HAase digestion before Western blot analysis. As shown in Fig. 6*C*, the anti-IαI antibody indeed revealed a major species of 80 kDa corresponding to the molecular mass of free HCs and a minor species of 35 kDa corresponding to bikunin of IαI and a HMW species in the loading well (Fig. 2*B*). HAase digestion resulted in an increase of the 80-kDa HCs species and the HMW smear but not the 35-kDa species, suggesting that the HMW species in the loading well was the HC-HA complex, which gave rise to the increased HCs following HAase digestion. These changes were not noted in the control using IgG, whereas the diffuse species at about 50 kDa (Fig. 6*C*, *open arrowhead*) corresponded to the heavy chains of rabbit IgG linked to Sepharose beads and eluted in the sample buffer. After stripping, the same blot reprobed with the anti-PTX3 antibody showed a 45-kDa species, a 90-kDa species, and an HMW species in the loading well, corresponding to the molecular masses of monomer PTX3, dimer PTX3, and the PTX3-containing complex, respectively. HAase digestion increased the 45-kDa and 90-kDa species and intensified the HMW PTX3 smear, suggesting that PTX3 was coimmunoprecipitated with HC-HA by anti-IαI antibody. These results confirmed the production of the HC-HA-PTX3 complex by AMSC cultures and the association of PTX3 with the HC-HA complex.

Effects of the HC-HA and HC-HA-PTX3 Complexes on Macrophage Phenotype—Our previous studies have shown that the HC-HA complex, purified from the AM, now the HC-HA-PTX3 complex, exerts the anti-inflammatory, antiscarring (21), and antiangiogenic (22) actions of the AM and can polarize macrophages to an M2 phenotype upon Toll-like receptor ligation (24). To determine whether the presence of PTX3 affects the biological function of the HC-HA complex, we first followed the reported methods (21, 32) to reconstitute the HC-HA complex (*i.e.* rcHC-HA) as well as the HC-HA-PTX3 complex (*i.e.* rcHC-HA-PTX3) by adding purified human IαI and recombinant humanTSG-6 with and without recombinant human PTX3 on HA covalently immobilized on a plastic surface. HC1 (Fig. 7*A*) and HC2 (Fig. 7*B*) ELISAs confirmed no transfer of HCs from purified IαI to immobilized HA in the absence of TSG-6. In contrast, both HC1 and HC2 were bound to immobilized HA when IαI was incubated with TSG-6, consistent with the formation of the rcHC-HA complex, as reported recently (32). Addition of PTX3 from 20–200 nM did not affect HC1 transfer to HA but dose-dependently increased HC2 transfer to HA ($p < 0.05$). Without immobilized HA, no HC1 or HC2 was detected, even when IαI, TSG-6, and PTX3 were incubated in the wells, confirming the formation of the rcHC-HA complex on the basis of the immobilized HA (32). TSG-6 binds to immobilized HA to form the TSG-6·HA com-

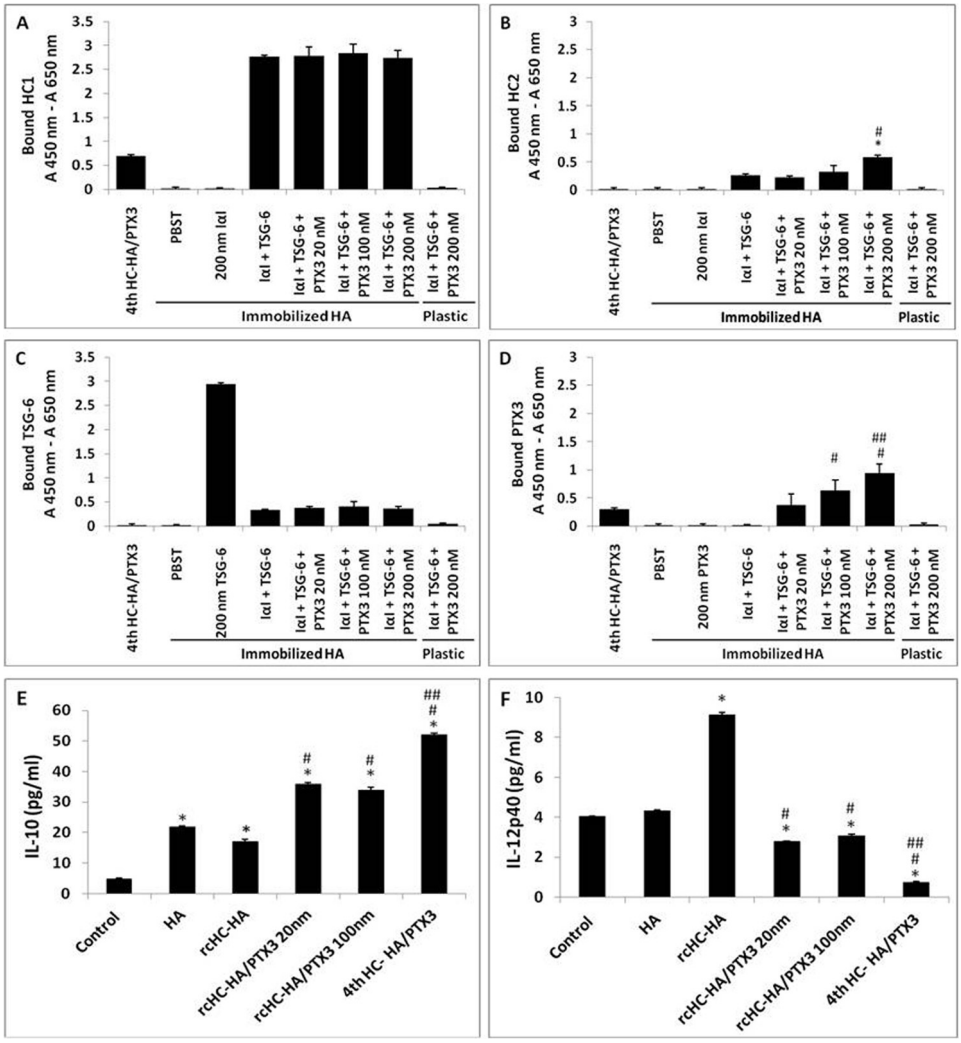

FIGURE 7. **Reconstitution of the HC-HA and HC-HA-PTX3 (rcHC-HA and rcHC-HA-PTX3) complexes *in vitro* and their effects on macrophage phenotype.** *A–D*, reconstitution of the rcHC-HA and rcHC-HA-PTX3 complexes *in vitro*. 2 μg of HA, AM fourth HC-HA/PTX3, or PBS control was covalently immobilized on the wells of a Covalink NH 96-well plate. After washing, the wells were blocked with 2% BSA in PBST at room temperature for 1 h. Thereafter, 200 nM IαI, 200 nM TSG-6, or 20–200 nM of PTX3 in PBST containing 5 mM $MgSO_4$ was added into the wells alone or together, as indicated, and incubated for 2 h at 37 °C. The wells were then washed with 6 M GnHCl before ELISA for the bound HC1 (*A*), HC2 (*B*), TSG-6 (*C*), and PTX3 (*D*) to immobilized HA, respectively. The results represent mean ± S.D. ($n = 4$). *, $p < 0.05$ for IαI + TSG-6 + PTX3 (200 nM) *versus* IαI + TSG-6; #, $p < 0.05$ for IαI + TSG-6 + PTX3 (100 or 200 nM) *versus* IαI + TSG-6 + PTX3 (20 nM); ##, $p < 0.05$ for IαI + TSG-6 + PTX3 (100 or 200 nM) *versus* IαI + TSG-6 + PTX3 (100 nM). *E* and *F*, RAW264.7 cells (3.1×10^4/cm^2) were seeded on the aforementioned rcHC-HA and rcHC-HA-PTX3 complexes and treated with 1 μg/ml LPS for 24 h. The protein levels of IL-10 (*E*) and IL-12p40 (*F*) were measured in conditioned medium by ELISA. The results represent mean ± S.D. ($n = 4$). *, $p < 0.01$ *versus* control; #, $p < 0.01$ *versus* rcHC-HA; ##, $p < 0.01$ *versus* rcHC-HA-PTX3 (20 or 100 nM).

plex, and both free and HA-bound TSG-6 can transfer HCs from IαI to immobilized HA to form rcHC-HA (32, 44). However, such binding of TSG-6 to immobilized HA is impaired in the presence of IαI (45). Consistent with these findings, we also noted that the amount of TSG-6 bound to immobilized HA greatly decreased when IαI was added together with TSG-6 to the immobilized HA compared with adding only TSG-6 to immobilized HA (Fig. 7*C*). Addition of PTX3 to IαI and TSG-6 did not further affect the binding of TSG-6 to HA when compared with no PTX3 addition. There was no binding of PTX3 to immobilized HA when PTX3 alone was incubated (Fig. 7*D*), in agreement with the finding that PTX3 does not directly bind to immobilized HA when HA coated the plate surface non-covalently (15). However, PTX3 was detected dose-dependently when PTX3 was incubated along with IαI and TSG-6 with immobilized HA from 20–200 nM (all $p < 0.05$). Collectively, these results suggest that PTX3 was bound to rcHC-HA and formed the rcHC-HA-PTX3 complex, presumably by interacting with HCs or TSG-6 (14, 15). We then seeded RAW264.7 murine macrophages on the aforementioned rcHC-HA and rcHC-HA-PTX3 complexes, challenged them with LPS for 24 h, and then measured the expression of IL-12 and IL-10 proteins as markers for the M1 and M2 phenotypes (46–48). The IL-10 protein level by ELISA was increased by rcHC-HA, rcHC-HA-PTX3, and AM fourth HC-HA-PTX3 (Fig. 7*E*). The extent of increase by rcHC-HA-PTX3 was higher than that by rcHC-HA but less than that by AM fourth HC-HA-PTX3 (all $p < 0.01$). In contrast, the IL-12p40 protein level was up-regulated by rcHC-HA ($p < 0.01$) but down-regulated by rcHC-HA-PTX3 and AM HC-HA-PTX3 (all $p < 0.01$). Such a down-regulation was more effective by AM HC-HA-PTX3 than by rcHC-HA-PTX3 formed by different PTX3 concentrations

($p < 0.01$). These results suggest that the presence of PTX3 in the rcHC-HA complex contributes to the polarization of M2 macrophages, similar to what has been reported for AM HC-HA-PTX3 (24).

DISCUSSION

The existence of PTX3 in the HC-HA complex was first demonstrated in the COC matrix surrounding the ovulated oocyte (14, 15). *Ptx3*-deficient mice are infertile because of instability of the cumulus matrix, although the formation of HC-HA complex is not impaired (15). It is believed that the stability of the HA-rich COC matrix depends on the binding of PTX3 to HCs of the HC-HA complex via the N-terminal domain (14). However, it remained unclear whether PTX3 is still associated with the HC-HA complex when the HC-HA complex is isolated and purified from the COC matrix in the same manner as demonstrated here. This study confirmed that PTX3 is also an integral component of the AM HC-HA complex. Positive PTX3 staining was reported in the amniotic epithelium, chorionic mesoderm, trophoblast terminal villi, and perivascular stroma of normal placentas (33). This finding endowed PTX3 with a presumptive role in preventing the presentation of apoptotic cell-associated antigens of the embryo to maternal T lymphocytes during pregnancy. Our immunostaining study, however, showed the predominant presence of PTX3 in the compact stroma of AM when compared with that of the AM epithelium and chorion (Fig. 1). Furthermore, a Western blot analysis showed that PTX3 was readily detected and tightly bound to the AM HC-HA complex, forming the HC-HA-PTX3 complex (Fig. 2). PTX3 was displayed as a multimeric form in the AM HC-HA-PTX3 complex despite reduction and alkylation. This property is different from what has been reported previously, *i.e.* that PTX3 is stabilized by a disulfide bond (1, 36). Hence, the AM is a tissue, other than the COC matrix, in which the HC-HA complex contains PTX3. The binding of PTX3 to AM HC-HA was strong to withstand four runs of ultracentrifugation in the presence of CsCl and 4 M GnHCl. The binding between PTX3 and HCs of IαI in the COC matrix has been demonstrated by coprecipitation of PTX3 with IαI-HCs with anti-IαI antibody or anti-PTX3 antibody from ovulated COC extracts and by direct binding of PTX3 to human serum-purified IαI in microtiter plates (14). It remains unclear whether HC1, HC2, or both are detected in the COC complex. However, HC1 alone is detected in the AM HC-HA complex (23, 24) (Fig. 2). Hence, further studies to determine how the aforementioned strong binding of PTX3 actually operates in the AM HC-HA complex will shed more light onto whether the HA-rich matrix in the AM during fetal development has a similar function to that of the COC complex in fertilization.

As expected, a low level of PTX3 mRNA and production of PTX3 protein were detected intracellularly, despite TNF or IL-1β treatment with or without FBS in HSF. Previous studies have shown constitutive expression of PTX3 protein by human neutrophils (stored in specific granules) (49), renal mesangial cells, and proximal tubular epithelial cells (50). Here we demonstrated that AM cells were another example that exhibited constitutive expression and secretion of PTX3, especially following treatment with TNF and IL-1β (Fig. 3). Consistent with earlier studies performed in cultured keratocytes (41, 42), an agarose overlay was effective in preventing the release of the HA-containing matrix into the culture medium (Fig. 4*A*), resembling entrapment of procollagens in the cell layer (41). This maneuver helped to restore a cell morphology more compatible with their *in vivo* counterparts (Fig. 4*B*). Another HC-HA complex, termed SHAP-HA, was first isolated from a cultured dermal fibroblast cell layer in the presence of FBS, and it contained both HC1 and HC2 derived from FBS (31, 40). Here we confirmed the presence of HC1 and HC2 in the cell layers of HSF in FBS after agarose overlay (Fig. 5). However, the presence of PTX3, HC1, and HC2 was noted in AMSC and AMEC even in the absence of FBS and TNF (Fig. 5). Western blot analysis confirmed the production of the HC-HA-PTX3 complex by AMSC, but not HSF, despite being cultured in the presence of FBS and under the stimulation of TNF (Fig. 6). These data are in agreement with our recent report that cultured AM cells produce the HC-HA complex in the cell layer using their endogenously generated IαI (23) and lead us to conclude that constitutive expression and release of PTX3 protein by AM cells led to the formation of the HC-HA-PTX3 complex. This notion was further substantiated by the production of an HMW PTX3 smear, a pattern found in the purified AM HC-HA-PTX3 complex, by exogenous application of recombinant PTX3 in HSF under agarose overlay in the presence of FBS (Fig. 6), which, as reported, generates the HC-HA complex (31, 40), and by the coimmunoprecipitation of PTX3 with HC-HA complex in agarose-overlaid AM cell cultures.

The presence of PTX3 in the AM HC-HA-PTX3 complex is responsible for the biological function of the AM HC-HA-PTX3 complex, as determined by polarization of LPS-treated macrophages to an M2 phenotype, with rcHC-HA-PTX3 being more potent than rcHC-HA. The HC-HA-PTX3 complex endogenously produced by AM may play an important protective role during fetal development and can be an active therapeutic agent. Further studies are needed to determine why both HC1 and HC2 were found in the HC-HA-PTX3 complex formed by cultured AM cells (Fig. 5) but only HC1 was found in that purified from the AM and whether such a unique composition is critical for the anti-inflammatory, antiscarring, and antiangiogenic actions of the AM during ocular surface reconstruction (51–54).

REFERENCES

1. Inforzato, A., Baldock, C., Jowitt, T. A., Holmes, D. F., Lindstedt, R., Marcellini, M., Rivieccio, V., Briggs, D. C., Kadler, K. E., Verdoliva, A., Bottazzi, B., Mantovani, A., Salvatori, G., and Day, A. J. (2010) The angiogenic inhibitor long pentraxin PTX3 forms an asymmetric octamer with two binding sites for FGF2. *J. Biol. Chem.* **285,** 17681–17692
2. Bottazzi, B., Doni, A., Garlanda, C., and Mantovani, A. (2010) An integrated view of humoral innate immunity: pentraxins as a paradigm. *Annu. Rev. Immunol.* **28,** 157–183
3. Inforzato, A., Jaillon, S., Moalli, F., Barbati, E., Bonavita, E., Bottazzi, B., Mantovani, A., and Garlanda, C. (2011) The long pentraxin PTX3 at the crossroads between innate immunity and tissue remodelling. *Tissue Antigens* **77,** 271–282
4. Manfredi, A. A., Rovere-Querini, P., Bottazzi, B., Garlanda, C., and Mantovani, A. (2008) Pentraxins, humoral innate immunity and tissue injury. *Curr. Opin. Immunol.* **20,** 538–544
5. Nauta, A. J., Daha, M. R., van Kooten, C., and Roos, A. (2003) Recognition and clearance of apoptotic cells: a role for complement and pentraxins. *Trends Immunol.* **24,** 148–154

6. Rovere, P., Peri, G., Fazzini, F., Bottazzi, B., Doni, A., Bondanza, A., Zimmermann, V. S., Garlanda, C., Fascio, U., Sabbadini, M. G., Rugarli, C., Mantovani, A., and Manfredi, A. A. (2000) The long pentraxin PTX3 binds to apoptotic cells and regulates their clearance by antigen-presenting dendritic cells. *Blood* **96,** 4300–4306
7. Garlanda, C., Bottazzi, B., Bastone, A., and Mantovani, A. (2005) Pentraxins at the crossroads between innate immunity, inflammation, matrix deposition, and female fertility. *Annu. Rev. Immunol.* **23,** 337–366
8. Garlanda, C., Hirsch, E., Bozza, S., Salustri, A., De Acetis, M., Nota, R., Maccagno, A., Riva, F., Bottazzi, B., Peri, G., Doni, A., Vago, L., Botto, M., De Santis, R., Carminati, P., Siracusa, G., Altruda, F., Vecchi, A., Romani, L., and Mantovani, A. (2002) Non-redundant role of the long pentraxin PTX3 in anti-fungal innate immune response. *Nature* **420,** 182–186
9. Han, B., Ma, X., Zhang, J., Zhang, Y., Bai, X., Hwang, D. M., Keshavjee, S., Levy, G. A., McGilvray, I., and Liu, M. (2012) Protective effects of long pentraxin PTX3 on lung injury in a severe acute respiratory syndrome model in mice. *Lab. Invest.* **92,** 1285–1296
10. Soares, A. C., Souza, D. G., Pinho, V., Vieira, A. T., Nicoli, J. R., Cunha, F. Q., Mantovani, A., Reis, L. F., Dias, A. A., and Teixeira, M. M. (2006) Dual function of the long pentraxin PTX3 in resistance against pulmonary infection with *Klebsiella pneumoniae* in transgenic mice. *Microbes Infect.* **8,** 1321–1329
11. Goodman, A. R., Cardozo, T., Abagyan, R., Altmeyer, A., Wisniewski, H. G., and Vilcek, J. (1996) Long pentraxins: an emerging group of proteins with diverse functions. *Cytokine Growth Factor Rev.* **7,** 191–202
12. Maina, V., Cotena, A., Doni, A., Nebuloni, M., Pasqualini, F., Milner, C. M., Day, A. J., Mantovani, A., and Garlanda, C. (2009) Coregulation in human leukocytes of the long pentraxin PTX3 and TSG-6. *J. Leukocyte Biol.* **86,** 123–132
13. Camozzi, M., Rusnati, M., Bugatti, A., Bottazzi, B., Mantovani, A., Bastone, A., Inforzato, A., Vincenti, S., Bracci, L., Mastroianni, D., and Presta, M. (2006) Identification of an antiangiogenic FGF2-binding site in the N terminus of the soluble pattern recognition receptor PTX3. *J. Biol. Chem.* **281,** 22605–22613
14. Scarchilli, L., Camaioni, A., Bottazzi, B., Negri, V., Doni, A., Deban, L., Bastone, A., Salvatori, G., Mantovani, A., Siracusa, G., and Salustri, A. (2007) PTX3 interacts with inter-α-trypsin inhibitor: implications for hyaluronan organization and cumulus oophorus expansion. *J. Biol. Chem.* **282,** 30161–30170
15. Salustri, A., Garlanda, C., Hirsch, E., De Acetis, M., Maccagno, A., Bottazzi, B., Doni, A., Bastone, A., Mantovani, G., Beck Peccoz, P., Salvatori, G., Mahoney, D. J., Day, A. J., Siracusa, G., Romani, L., and Mantovani, A. (2004) PTX3 plays a key role in the organization of the cumulus oophorus extracellular matrix and in *in vivo* fertilization. *Development* **131,** 1577–1586
16. Fülöp, C., Szántó, S., Mukhopadhyay, D., Bárdos, T., Kamath, R. V., Rugg, M. S., Day, A. J., Salustri, A., Hascall, V. C., Glant, T. T., and Mikecz, K. (2003) Impaired cumulus mucification and female sterility in tumor necrosis factor-induced protein-6 deficient mice. *Development* **130,** 2253–2261
17. Jessen, T. E., and Ødum, L. (2003) Role of tumour necrosis factor stimulated gene 6 (TSG-6) in the coupling of inter-α-trypsin inhibitor to hyaluronan in human follicular fluid. *Reproduction.* **125,** 27–31
18. Rugg, M. S., Willis, A. C., Mukhopadhyay, D., Hascall, V. C., Fries, E., Fülöp, C., Milner, C. M., and Day, A. J. (2005) Characterization of complexes formed between TSG-6 and inter-α-inhibitor that act as intermediates in the covalent transfer of heavy chains onto hyaluronan. *J. Biol. Chem.* **280,** 25674–25686
19. Sato, H., Kajikawa, S., Kuroda, S., Horisawa, Y., Nakamura, N., Kaga, N., Kakinuma, C., Kato, K., Morishita, H., Niwa, H., and Miyazaki, J. (2001) Impaired fertility in female mice lacking urinary trypsin inhibitor. *Biochem. Biophys. Res. Commun.* **281,** 1154–1160
20. Zhuo, L., Yoneda, M., Zhao, M., Yingsung, W., Yoshida, N., Kitagawa, Y., Kawamura, K., Suzuki, T., and Kimata, K. (2001) Defect in SHAP-hyaluronan complex causes severe female infertility: a study by inactivation of the bikunin gene in mice. *J. Biol. Chem.* **276,** 7693–7696
21. He, H., Li, W., Tseng, D. Y., Zhang, S., Chen, S. Y., Day, A. J., and Tseng, S. C. (2009) Biochemical characterization and function of complexes formed by hyaluronan and the heavy chains of inter-α-inhibitor (HC·HA) purified from extracts of human amniotic membrane. *J. Biol. Chem.* **284,** 20136–20146
22. Shay, E., He, H., Sakurai, S., and Tseng, S. C. (2011) Inhibition of angiogenesis by HC·HA, a complex of hyaluronan and the heavy chain of inter-α-inhibitor, purified from human amniotic membrane. *Invest Ophthalmol. Vis. Sci.* **52,** 2669–2678
23. Zhang, S., He, H., Day, A. J., and Tseng, S. C. (2012) Constitutive expression of inter-α-inhibitor (IαI) family proteins and tumor necrosis factor-stimulated gene-6 (TSG-6) by human amniotic membrane epithelial and stromal cells supporting formation of the heavy chain-hyaluronan (HC-HA) complex. *J. Biol. Chem.* **287,** 12433–12444
24. He, H., Zhang, S., Tighe, S., Son, J., and Tseng, S. C. (2013) Immobilized HC-HA polarizes LPS-activated macrophages toward M2 phenotype. *J. Biol. Chem.* **288,** 25792–25803
25. Blom, A. M., Mörgelin, M., Oyen, M., Jarvet, J., and Fries, E. (1999) Structural characterization of inter-α-inhibitor: evidence for an extended shape. *J. Biol. Chem.* **274,** 298–304
26. Muramatu, M., Mori, S., Matsuzawa, Y., Horiguchi, Y., Nakanishi, Y., and Tanaka, M. (1980) Purification and characterization of urinary trypsin inhibitor, UTI68, from normal human urine, and its cleavage by human uropepsin. *J. Biochem.* **88,** 1317–1329
27. Chen, Y. T., Li, W., Hayashida, Y., He, H., Chen, S. Y., Tseng, D. Y., Kheirkhah, A., and Tseng, S. C. (2007) Human amniotic epithelial cells as novel feeder layers for promoting *ex vivo* expansion of limbal epithelial progenitor cells. *Stem Cells* **25,** 1995–2005
28. Li, W., He, H., Chen, Y. T., Hayashida, Y., and Tseng, S. C. (2008) Reversal of myofibroblasts by amniotic membrane stromal extract. *J. Cell. Physiol.* **215,** 657–664
29. Chen, S. Y., Hayashida, Y., Chen, M. Y., Xie, H. T., and Tseng, S. C. (2011) A new isolation method of human limbal progenitor cells by maintaining close association with their niche cells. *Tissue Eng. Part C Methods* **17,** 537–548
30. He, H., Li, W., Chen, S. Y., Zhang, S., Chen, Y. T., Hayashida, Y., Zhu, Y. T., and Tseng, S. C. (2008) Suppression of activation and induction of apoptosis in RAW264.7 cells by amniotic membrane extract. *Invest. Ophthalmol. Vis. Sci.* **49,** 4468–4475
31. Yoneda, M., Suzuki, S., and Kimata, K. (1990) Hyaluronic acid associated with the surfaces of cultured fibroblasts is linked to a serum-derived 85-kDa protein. *J. Biol. Chem.* **265,** 5247–5257
32. Colón, E., Shytuhina, A., Cowman, M. K., Band, P. A., Sanggaard, K. W., Enghild, J. J., and Wisniewski, H. G. (2009) Transfer of inter-α-inhibitor heavy chains to hyaluronan by surface-linked hyaluronan-TSG-6 complexes. *J. Biol. Chem.* **284,** 2320–2331
33. Rovere-Querini, P., Antonacci, S., Dell'Antonio, G., Angeli, A., Almirante, G., Cin, E. D., Valsecchi, L., Lanzani, C., Sabbadini, M. G., Doglioni, C., Manfredi, A. A., and Castiglioni, M. T. (2006) Plasma and tissue expression of the long pentraxin 3 during normal pregnancy and preeclampsia. *Obstet. Gynecol.* **108,** 148–155
34. Jessen, T. E., Odum, L., and Johnsen, A. H. (1994) *In vivo* binding of human inter-α-trypsin inhibitor free heavy chains to hyaluronic acid. *Biol. Chem. Hoppe-Seyler* **375,** 521–526
35. Zhao, M., Yoneda, M., Ohashi, Y., Kurono, S., Iwata, H., Ohnuki, Y., and Kimata, K. (1995) Evidence for the covalent binding of SHAP, heavy chains of inter-α-trypsin inhibitor, to hyaluronan. *J. Biol. Chem.* **270,** 26657–26663
36. Inforzato, A., Rivieccio, V., Morreale, A. P., Bastone, A., Salustri, A., Scarchilli, L., Verdoliva, A., Vincenti, S., Gallo, G., Chiapparino, C., Pacello, L., Nucera, E., Serlupi-Crescenzi, O., Day, A. J., Bottazzi, B., Mantovani, A., De Santis, R., and Salvatori, G. (2008) Structural characterization of PTX3 disulfide bond network and its multimeric status in cumulus matrix organization. *J. Biol. Chem.* **283,** 10147–10161
37. Lee, G. W., Lee, T. H., and Vilcek, J. (1993) TSG-14, a tumor necrosis factor- and IL-1-inducible protein, is a novel member of the pentaxin family of acute phase proteins. *J. Immunol.* **150,** 1804–1812
38. Lee, T. H., Lee, G. W., Ziff, E. B., and Vilcek, J. (1990) Isolation and characterization of eight tumor necrosis factor-induced gene sequences from human fibroblasts. *Mol. Cell. Biol.* **10,** 1982–1988

39. Luchetti, M. M., Sambo, P., Majlingová, P., Svegliati Baroni, S., Peri, G., Paroncini, P., Introna, M., Stoppacciaro, A., Mantovani, A., and Gabrielli, A. (2004) Scleroderma fibroblasts constitutively express the long pentraxin PTX3. *Clin. Exp. Rheumatol.* **22,** S66–S72
40. Huang, L., Yoneda, M., and Kimata, K. (1993) A serum-derived hyaluronan-associated protein (SHAP) is the heavy chain of the inter α-trypsin inhibitor. *J. Biol. Chem.* **268,** 26725–26730
41. Hassell, J. R., Kane, B. P., Etheredge, L. T., Valkov, N., and Birk, D. E. (2008) Increased stromal extracellular matrix synthesis and assembly by insulin activated bovine keratocytes cultured under agarose. *Exp. Eye Res.* **87,** 604–611
42. Etheredge, L., Kane, B. P., Valkov, N., Adams, S., Birk, D. E., and Hassell, J. R. (2010) Enhanced cell accumulation and collagen processing by keratocytes cultured under agarose and in media containing IGF-I, TGF-β or PDGF. *Matrix Biol.* **29,** 519–524
43. Yingsung, W., Zhuo, L., Morgelin, M., Yoneda, M., Kida, D., Watanabe, H., Ishiguro, N., Iwata, H., and Kimata, K. (2003) Molecular heterogeneity of the SHAP-hyaluronan complex: isolation and characterization of the complex in synovial fluid from patients with rheumatoid arthritis. *J. Biol. Chem.* **278,** 32710–32718
44. Wisniewski, H. G., Snitkin, E. S., Mindrescu, C., Sweet, M. H., and Vilcek, J. (2005) TSG-6 protein binding to glycosaminoglycans: formation of stable complexes with hyaluronan and binding to chondroitin sulfates. *J. Biol. Chem.* **280,** 14476–14484
45. Baranova, N. S., Foulcer, S. J., Briggs, D. C., Tilakaratna, V., Enghild, J. J., Milner, C. M., Day, A. J., and Richter, R. P. (2013) Inter-α-inhibitor impairs TSG-6-induced hyaluronan cross-linking. *J. Biol. Chem.* **288,** 29642–29653
46. Anderson, C. F., and Mosser, D. M. (2002) A novel phenotype for an activated macrophage: the type 2 activated macrophage. *J. Leukocyte Biol.* **72,** 101–106
47. Edwards, J. P., Zhang, X., Frauwirth, K. A., and Mosser, D. M. (2006) Biochemical and functional characterization of three activated macrophage populations. *J. Leukocyte Biol.* **80,** 1298–1307
48. Mosser, D. M. (2003) The many faces of macrophage activation. *J. Leukocyte Biol.* **73,** 209–212
49. Jaillon, S., Peri, G., Delneste, Y., Frémaux, I., Doni, A., Moalli, F., Garlanda, C., Romani, L., Gascan, H., Bellocchio, S., Bozza, S., Cassatella, M. A., Jeannin, P., and Mantovani, A. (2007) The humoral pattern recognition receptor PTX3 is stored in neutrophil granules and localizes in extracellular traps. *J. Exp. Med.* **204,** 793–804
50. Nauta, A. J., de Haij, S., Bottazzi, B., Mantovani, A., Borrias, M. C., Aten, J., Rastaldi, M. P., Daha, M. R., van Kooten, C., and Roos, A. (2005) Human renal epithelial cells produce the long pentraxin PTX3. *Kidney Int.* **67,** 543–553
51. Bouchard, C. S., and John, T. (2004) Amniotic membrane transplantation in the management of severe ocular surface disease: indications and outcomes. *Ocul. Surf.* **2,** 201–211
52. Dua, H. S., Gomes, J. A., King, A. J., and Maharajan, V. S. (2004) The amniotic membrane in ophthalmology. *Surv. Ophthalmol.* **49,** 51–77
53. Tseng, S. C. (2001) Amniotic membrane transplantation for ocular surface reconstruction. *Biosci. Rep.* **21,** 481–489
54. Tseng, S. C., Espana, E. M., Kawakita, T., Di Pascuale, M. A., Li, W., He, H., Liu, T. S., Cho, T. H., Gao, Y. Y., Yeh, L. K., and Liu, C. Y. (2004) How does amniotic membrane work? *Ocul. Surf.* **2,** 177–187